Neurosci. Bull. December, 2024, 40(12):1955–1959
https://doi.org/10.1007/s12264-024-01271-6

www.neurosci.cn
www.springer.com/12264

LETTER TO THE EDITOR

Context-dependent Grid-like Representations of Theta Power in Human Entorhinal Cortex

Pengcheng Lv[1,2] · Dong Chen[1,2] · Hui Zhang[3] · Wenjing Zhou[4] · Mengyang Wang[5] · Philip Grewe[7,8] · Nikolai Axmacher[3,6] · Liang Wang[1,2]

Received: 31 January 2024 / Accepted: 2 April 2024 / Published online: 7 August 2024
© Center for Excellence in Brain Science and Intelligence Technology, Chinese Academy of Sciences 2024

Dear Editor,

Electrophysiological studies have found that the entorhinal cortex (EC) contains grid cells that fire at the vertices of equilateral triangles tiling the entire environment [1–3]. Theoretical models [4] and empirical studies [5] suggest that they are a key neural substrate for spatial navigation. In humans, grid cells can be indirectly measured by grid-like representations (GLRs) at the level of fMRI BOLD responses [6] and local field potentials [7]. Rodent studies have demonstrated that grid orientations are modulated by environment cues and tend to align to boundaries [8] and distal cues [1]. By contrast, proximal cues such as objects [9] and walls [10] within areas disrupt the firing patterns of grid cells. Similar effects of boundary cues have also been reported on human GLRs [11, 12]. However, it is unclear whether GLRs in human EC are influenced by salient proximal cues. Firstly, considering the relevance of grid cells and theta oscillations [13], we hypothesized that theta power in the EC showed a GLR, as in previous studies [7]. Secondly, we hypothesized that proximal cues significantly altered GLR patterns. To address these questions, we recruited drug-resistant epilepsy patients with implanted depth electrodes to perform a virtual navigation task in environments with varying cues (Fig. 1A, B).

Firstly, we compared the drop error to chance performance (i.e., surrogate distributions; Fig. S1B, C; for details see "Supplementary Materials"). We found that the behavioral performance was significantly higher than the chance level (one-sample t-test against 0.5, $t_8 = 23.34$, $P < 0.001$; Fig. 1C), indicating that patients performed the task well.

Next, we explored GLRs in the EC during the navigation task (Fig. 1D, E). Considering the dependence of contacts within the same patient, this analysis was conducted using linear mixed-effects models (LMEs) in 5 patients with 17 EC contacts. As in previous studies, we restricted our analyses to fast movement periods in which GLRs are most prominent [6, 7]. We confirmed that movement directions were uniformly sampled across the 360° range (Rayleigh's tests, all P values >0.99; Fig. S2A-I). We then extracted the power

Pengcheng Lv and Dong Chen contributed equally to this work.

Supplementary Information The online version contains supplementary material available at https://doi.org/10.1007/s12264-024-01271-6.

✉ Liang Wang
lwang@psych.ac.cn

1 CAS Key Laboratory of Mental Health, Institute of Psychology, Beijing 100101, China

2 Department of Psychology, University of Chinese Academy of Sciences, Beijing 101408, China

3 Department of Neuropsychology, Institute of Cognitive Neuroscience, Faculty of Psychology, Ruhr University Bochum, 44801 Bochum, Germany

4 Department of Epilepsy Center, Tsinghua University Yuquan Hospital, Beijing 100039, China

5 Sanbo Brain Hospital, Capital Medical University, Beijing 100093, China

6 State Key Laboratory of Cognitive Neuroscience and Learning and IDG, McGovern Institute for Brain Research, Beijing Normal University, Beijing 100875, China

7 Clinical Neuropsychology and Epilepsy Research, Medical School OWL, Bielefeld University, 33615 Bielefeld, Germany

8 Department of Epileptology, Medical School, Mara Hospital (Bethel Epilepsy Center), Bielefeld University, 33617 Bielefeld, Germany

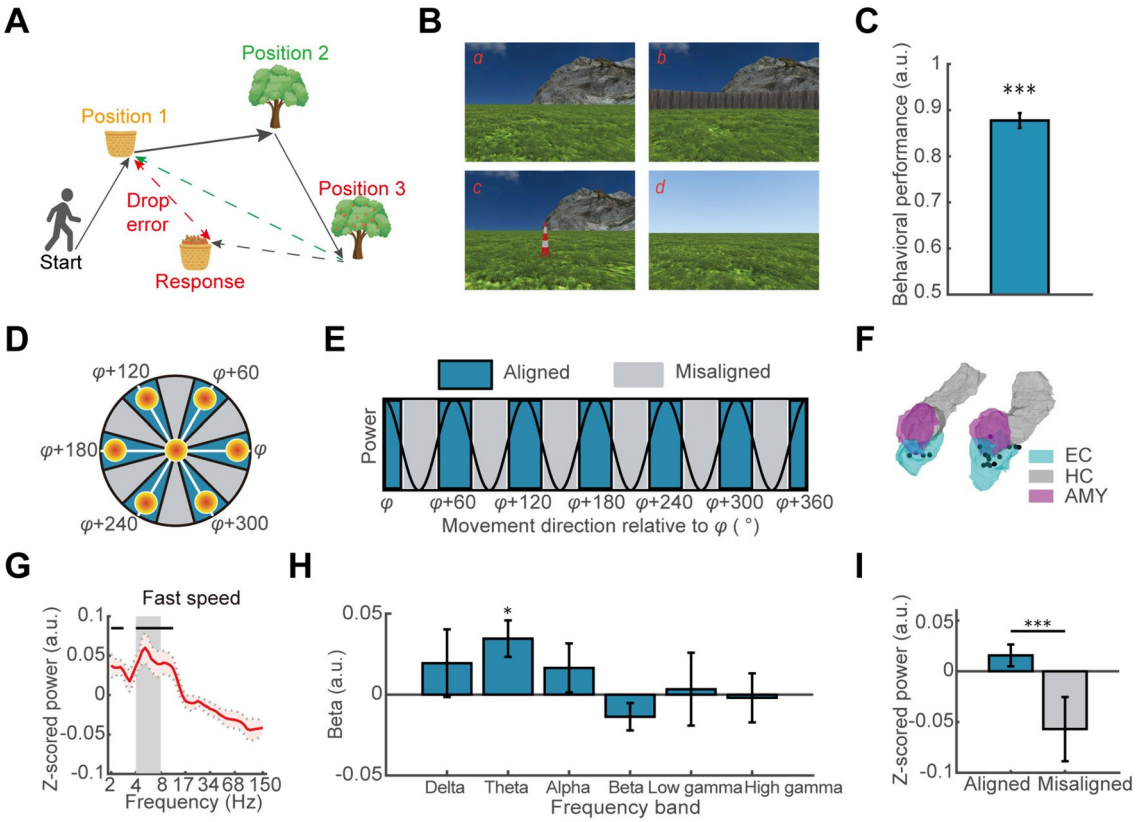

Fig. 1 Task and GLRs in the EC. **A** Schematic of the triangle completion task (for details see Supplementary Materials). **B** Four virtual environments with different external cues. Environment *a* - only distal cues. Environment *b* - distal cues and boundary. Environment *c* - distal cues and proximal cues. Environment *d* - no environmental cues. **C** Behavioral performance of participants. Error bars indicate the standard error of the mean (SEM) across patients. **D** Schematic of GLR analysis. A grid cell tiles the environment with hexadirectional firing fields (yellow dots). According to the grid orientation φ, the movement directions can be divided into aligned (blue) and misaligned (gray) movements. **E** Due to the hexadirectional symmetry of grid orientations, oscillatory power is higher when moving along the aligned direction compared to the misaligned direction. **F** Three regions of interest (EC, entorhinal cortex; HC, hippocampus; AMY, amygdala). EC contacts are shown as black dots. **G** Power spectrum during fast movements. Black lines indicate frequencies in which the power is significantly greater than zero (P <0.05, FDR corrected). The theta band (4-8 Hz) is highlighted in shaded gray areas. **H** The magnitude of GLRs across six frequency bands. **I** Theta power during fast movements along the aligned and misaligned directions. **G-I** Y-axes show the values estimated from the corresponding LMEs. Error bars indicate the SEM estimated from LMEs. *P <0.05, ***P <0.001 (FDR corrected).

spectrum of EC contacts, which showed a significant peak in the theta band (peak at 5.27 Hz; $t_{16} = 3.109$, $P = 0.007$, FDR corrected; Fig. 1G).

For the subsequent analysis of GLRs, we focused on the theta band (4–8 Hz) and took five additional bands as controls (delta, 1–4 Hz; alpha, 8–13 Hz; beta, 13–30 Hz; low gamma, 30–80 Hz; and high gamma, 80–150 Hz). We divided the concatenated fast movement epochs of each patient into 6 sessions. For half of the data, we fitted the time course of theta power with a general linear model (GLM1) consisting of two regressors that were a pair of sine and cosine regressors depending on movement directions with a period of 60°. The β values of these regressors were then used to calculate the preferred direction φ. For the other half of the data, theta power was fitted by another general linear model (GLM2) that consisted of a cosine regressor of the difference between the instantaneous movement direction and the preferred direction, again in 60° space. This analysis revealed a significant GLR in the theta band ($t_{16} = 3.074$, $P = 0.044$, FDR corrected; Fig. 1H) but not in other bands (all t_{16} <1.09, all P >0.37, FDR corrected; Fig. 1H). In a more direct comparison, we found that theta power was significantly greater during the aligned *versus* the misaligned movements ($t_{32} = 6.742$, P <0.001; Fig. 1I). Since only two patients completed the task of environment *d*, to ensure the consistency of data of all patients, we removed the data of environment *d* of these patients and conducted the above analysis again, which yielded similar results.

We also conducted several control analyses. No significant GLRs were found at medium speed ($t_{16} = 0.974$, $P = 0.345$) or slow ($t_{16} = -0.817$, $P = 0.426$; Fig. S3A) movements. We also tested whether EC theta power was

modulated by movement direction at 4-, 5-, 7-, or 8-fold rotational symmetry. None of these reached significance (all t_{16} <0.835, all P >0.152; Fig. S3B). Finally, we selected contacts located in the hippocampus (55 contacts across 8 patients) and amygdala (34 contacts across 5 patients) that were adjacent to the EC and analyzed whether their theta power showed GLRs. No significant GLRs were found in these two regions (hippocampus: $t_{54} = 0.512$, $P = 0.611$; amygdala: $t_{33} = -0.155$, $P = 0.877$; Fig. S3C).

In summary, we showed theta-based GLRs in a navigation task, consistent with previous findings, demonstrating its robustness. Next, we investigated how environmental cues affected human GLRs. Previous studies have found that external cues can influence the performance of navigation tasks [14]. We thus examined the performance differences in environments *a*, *b*, and *c*. Given that the number of participants who completed environment *d* did not match the first three environments, we removed the data from environment *d* in the subsequent analysis. Since the center of the circular boundary coincides with the landmark in environment *c*, the distance between the target location and the center of the environment ($D_{Target-to-center}$) in each trial may affect behavioral performance. Therefore, when comparing participants' behavioral performance in the three environments, we applied an LME of trial-wise performance with (1) $D_{Target-to-center}$, (2) environment category, (3) the interaction between these terms as fixed factors, and (4) participant as a random factor.

We found a main effect of the environment category ($F_{(2,570)} = 22.03$, P <0.001). Post-hoc pair-wise comparisons showed that performance in environments *b* and *c* was significantly better than in *a* (all P <0.001, FDR corrected; Fig. 2A). More importantly, we found an interaction between environment and $D_{Target-to-center}$ ($F_{(2,570)} = 4.464$, $P = 0.012$; Fig. 2B). Post hoc comparisons revealed that the performance in environments *a* and *b* increased more strongly with increasing $D_{Target-to-center}$ than the performance in environment *c* (slope of environment *a vs c*: $P = 0.017$, the slope of environment *b vs c*: $P = 0.017$, FDR corrected; Fig. 2B). These results did not change substantially even when the data were limited to the group of five patients with EC contacts (Fig. S4).

Furthermore, we determined whether the GLRs were affected by external cues. For example, for environments *a* and *b* (Fig. 2C), we used the data of environment *a* as the training set and the data of environment *b* as the test set to obtain $\beta_{a\to b}$. Then, we swapped the data of the training set and test set to obtain $\beta_{b\to a}$. We averaged $\beta_{a\to b}$ and $\beta_{b\to a}$ to measure the grid consistency of environments *a* and *b* (i.e., $\beta_{a\leftrightarrow b}$) (Fig. 2C). We applied the same procedure to environments *a* and *c* and environments *b* and *c*. The results showed that there were differences in the grid consistency among the

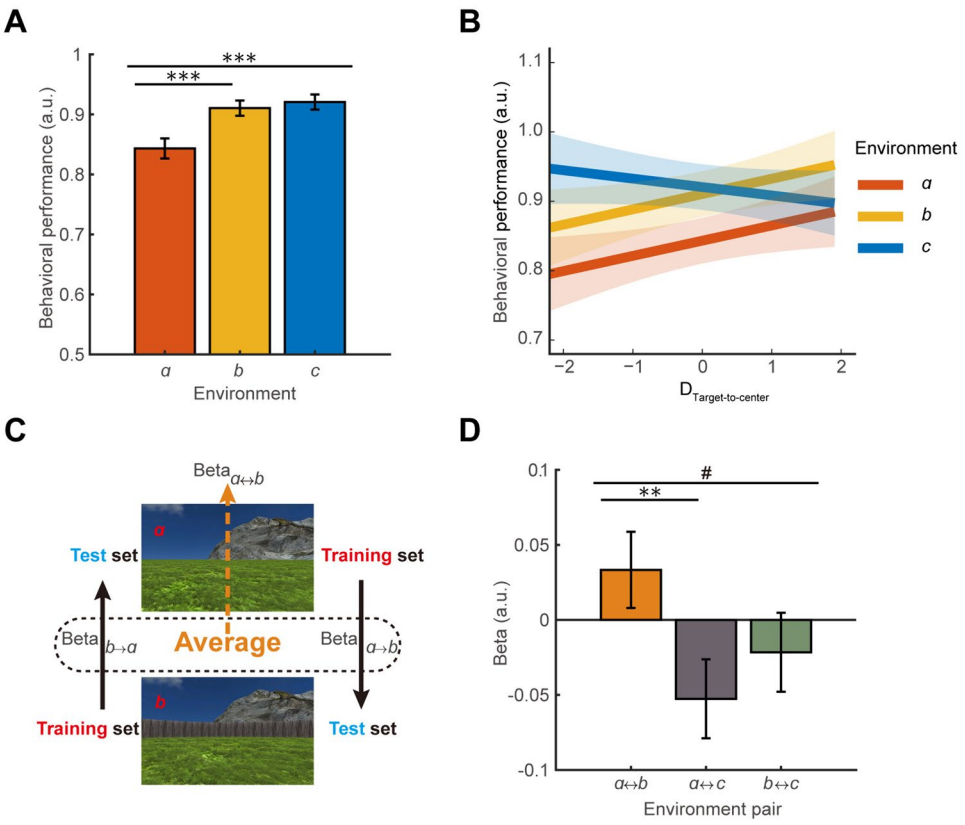

Fig. 2 Consistency of grid orientations between environments. **A** Differences in performance across the three environments. **B** The distance between the target location and the center of the environment ($D_{Target-to-center}$) had different influences on behavioral performance in the three environments. **C** Schematic for calculating the consistency of orientations of GLRs between environment *a* and environment *b*. **D** Consistency of GLR of the three environment pairs. Y-axes show the values estimated from the corresponding LMEs. Error bars indicate the SEM estimated from LMEs. $^{\#}P$ <0.1, $^{**}P$ <0.01, $^{***}P$ <0.001 (FDR corrected).

three environment pairs ($F_{(2,48)} = 5.473$, $P = 0.007$). Post hoc comparison found that $\beta_{a\leftrightarrow b}$ was significantly greater than $\beta_{a\leftrightarrow c}$ ($P = 0.006$, FDR corrected; Fig. 2D). Although not surviving multiple comparisons correction, $\beta_{a\leftrightarrow b}$ also tended to be larger than $\beta_{b\leftrightarrow c}$ ($P = 0.063$, FDR corrected; Fig. 2D). We examined the theta power of different environments and found no differences between them ($F_{(2,48)} = 0.554$, $P = 0.578$; Fig. S5A), indicating that the difference in grid consistencies was not caused by theta power differences between environments.

Considering that we detected significant GLRs in data with three environments (Fig. 1H), and subsequent results showed that only the grid orientations of environment *a* and environment *b* were more consistent (Fig. 2D), we speculated that the main contribution to the results of all data might come from environments *a* and *b*. So, we directly determined whether the grid orientation in each environment matched the grid orientation across all data. The results showed that only the grid orientations of environment *a* (V test, $v = 10.64$, $P < 0.001$; Fig. S5B) and environment *b* (V test, $v = 8.94$, $P = 0.001$; Fig. S5C) matched the grid orientation of all data, while the grid orientation of environment *c* tended to be different from the grid orientation of all data (V test, $v = 4.0$, $P = 0.08$; Fig. S5D).

Compared with environment *a*, the boundary in environment *b* generally improved navigation performance, regardless of the distance from the target to the boundary. By contrast, the landmark in environment *c* only improved the behavioral performance in trials in which the target location was closer to the landmark. These results support the view that boundary cues and landmark cues influence navigation behavior in different ways. Previous studies have shown that boundary-related learning is incidental, and associated with hippocampal activity, whereas landmark-based learning obeys associative reinforcement, and is associated with activity in the striatum [15].

Although environment *c* had the same distal cues as environments *a* and *b*, the grid orientation was less consistent, putatively due to the presence of a salient proximal cue. Our results showed that only grid orientations of environments *a* and *b* were close to the grid orientation across all data. Two reasons may account for those results. First, a GLR could still be formed in environment *c*, but the grid orientation may have been changed due to the influence of the local landmark, and no longer anchored to the same distal cues. Second, the proximal cues may have promoted the participants to use alternative navigational strategies that did not rely on path integration, and thus GLRs may be less pronounced in this environment. To support this view, a human fMRI study has found that a navigation strategy based on local landmarks depends on the function of the striatum rather than the medial temporal lobe [15]. In another fMRI study, it was found that, compared to a path integration subtask without any external cues, the activity of the retrosplenial cortex was stronger when completing path integration with landmark cues [14] (see Supplementary Notes 2 and 3 for further discussion).

In this study, we confirmed that theta power in the EC was hexadirectionally modulated by movement direction. Moreover, grid orientations were consistent between two environments with or without a boundary but were disrupted in the presence of a local landmark. In conclusion, this study provides direct electrophysiological evidence of context-dependent grid-like representations in the human entorhinal cortex.

Acknowledgements We are grateful to the participants in our study. This work was supported by STI2030-Major Projects (2022ZD0205000), the National Natural Science Foundation of China (32020103009 and 32200861), and a Ministry Key Project (GW0890006). NA acknowledges funding via DFG grant Project number 429281110. P.G. holds the Friedrich von Bodelschwingh Endowed Junior-Professorship for Clinical Neuropsychology and Epilepsy Research at the Medical School OWL, Bielefeld University, Germany funded by the v. Bodelschwingh Foundation.

Data availability The datasets generated during and/or analyzed during the current study are available from the corresponding author upon reasonable request.

Conflict of interest The authors declare that there are no conflicts of interest.

References

1. Hafting T, Fyhn M, Molden S, Moser MB, Moser EI. Microstructure of a spatial map in the entorhinal cortex. Nature 2005, 436: 801–806.
2. Jacobs J, Weidemann CT, Miller JF, Solway A, Burke JF, Wei XX. Direct recordings of grid-like neuronal activity in human spatial navigation. Nat Neurosci 2013, 16: 1188–1190.
3. Long X, Tao Y, Chen XC, Deng B, Cai J, Zhang SJ. Getting lost: Place cells and grid cells in rodent models of Alzheimer's disease. Neurosci Bull 2021, 37: 894–897.
4. McNaughton BL, Battaglia FP, Jensen O, Moser EI, Moser MB. Path integration and the neural basis of the 'cognitive map.' Nat Rev Neurosci 2006, 7: 663–678.
5. Gil M, Ancau M, Schlesiger MI, Neitz A, Allen K, De Marco RJ, *et al*. Impaired path integration in mice with disrupted grid cell firing. Nat Neurosci 2018, 21: 81–91.
6. Doeller CF, Barry C, Burgess N. Evidence for grid cells in a human memory network. Nature 2010, 463: 657–661.
7. Chen D, Kunz L, Wang W, Zhang H, Wang WX, Schulze-Bonhage A, *et al*. Hexadirectional modulation of *Theta* power in human entorhinal cortex during spatial navigation. Curr Biol 2018, 28: 3310-3315.e4.
8. Krupic J, Bauza M, Burton S, Barry C, O'Keefe J. Grid cell symmetry is shaped by environmental geometry. Nature 2015, 518: 232–235.
9. Boccara CN, Nardin M, Stella F, O'Neill J, Csicsvari J. The entorhinal cognitive map is attracted to goals. Science 2019, 363: 1443–1447.

10. Derdikman D, Whitlock JR, Tsao A, Fyhn M, Hafting T, Moser MB, *et al*. Fragmentation of grid cell maps in a multicompartment environment. Nat Neurosci 2009, 12: 1325–1332.
11. He Q, Brown TI. Environmental barriers disrupt grid-like representations in humans during navigation. Curr Biol 2019, 29: 2718-2722.e3.
12. Julian JB, Doeller CF. Remapping and realignment in the human hippocampal formation predict context-dependent spatial behavior. Nat Neurosci 2021, 24: 863–872.
13. Brandon MP, Bogaard AR, Libby CP, Connerney MA, Gupta K, Hasselmo ME. Reduction of *Theta rhythm* dissociates grid cell spatial periodicity from directional tuning. Science 2011, 332: 595–599.
14. Bierbrauer A, Kunz L, Gomes CA, Luhmann M, Deuker L, Getzmann S, *et al*. Unmasking selective path integration deficits in Alzheimer's disease risk carriers. Sci Adv 2020, 6: eaba1394.
15. Doeller CF, King JA, Burgess N. Parallel striatal and hippocampal systems for landmarks and boundaries in spatial memory. Proc Natl Acad Sci U S A 2008, 105: 5915–5920.